Electrostrictive thin films for RF acoustic resonators

Sylvia Sanchez , Gwenaël Le Rhun, Aurélien Suhm, Christophe Billard, Denis Mercier, Emmanuel Defaÿ

CEA LETI, Minatec, Grenoble, France

gwenael.le-rhun@cea.fr

edefay@cea.fr

***Abstract*— This paper describes the realisation and characterization of Bulk Acoustic wave resonators by using (Ba,Sr)TiO_3 (BST) as active material. As BST is electrostrictive, it requires a dc voltage to exhibit an electromechanical coupling. Resonances variations versus the dc field are observed and analyzed by using an analytical model based on acoustic propagation. This study proves that BST can exhibit a high electromechanical coupling reaching 8.5% which is higher than Aluminium Nitride, the standard material for acoustic resonators in the GHz frequency range. Moreover, this simple test vehicle allows extracting the frequency variation experienced by BST. Due to non negligible second order effects as electrostriction, dielectric and stiffness non linearities, these tunable features are highly desirable for tunable filters. A final simulation shows that tunable passband filters could be obtained by using BST based resonators.**

I. INTRODUCTION

Aluminium nitride (AlN) is the most popular material for thin films bulk acoustic resonators (FBAR) as it gathers an interesting electromechanical coupling ($k_t^2=7\%$) and low acoustical losses as the resonance quality factor can reach values higher than 1000. It is mainly used to synthesize RF filters in the front end modules of mobile phones. However, some communication standards require broader bandwidths. This induces higher coupling coefficients if acoustical resonators are used. Besides, it can be interesting to adjust the central frequency of filters in order to skip one channel to another one or to adjust technological drifts in the resonance frequency of resonators. Both features cannot be obtained by using AlN as its k_t^2 is already optimal and AlN does not exhibit large frequency agility versus dc field. Electrostrictive materials are a convincing alternative to AlN in order to address the tunable and large bandwidth issues. Indeed, (Ba,Sr)TiO_3 (BST), one of the most interesting electrostrictive material, can exhibit interesting values around 6% for k_t^2 [1] and also frequency variations reaching quite 2% for the resonance frequency [2]. These features are obtained by superimposing a dc field to the rf supply. Therefore, the dc field induces variations of the electromechanical properties of the electrostrictive material which in turn changes the resonance and antiresonance frequencies of the resonator. In this paper, we detail the realisation and the rf characterization of BST resonators together with an acoustical model. The extracted data are used to model the behaviour of a one-stage ladder filter versus dc field applied to the electrostrictive resonators.

II. TECHNOLOGY

Figure 1 is a sketch of the technology developed in this study. A 200mm silicon substrate is first thermally oxidized on 500nm. An adhesive layer made of TiO_2 10nm-thick is deposited by sputtering followed by the deposition in the same apparatus of Pt 100nm-thick at 400°C. Therefore, BST (Ba/Sr=70/30) is deposited by sol gel. This technique is a spinning of a solution which is a mix of BST precursors together with a solvent. The spinning step is followed by a solvent evaporation on a hot plate at 110°C. The sol gel layer is then dried between 300°C and 400°C in order to evacuate all the carbon-based species inside the layer. These three-steps are then repeated several times in order to increase the final thickness. One should note that it is mandatory to anneal the wafer at 700°C under air after three layers depositions in order to let BST crystallize in the desired perovskite phase. This annealing process can be done by classical annealing or by rapid Thermal Annealing. The tested devices here exhibit a final thickness of 300nm obtained after 8 depositions. Finally, the Pt top electrode 100nm-thick is sputtered and patterned by ion milling.

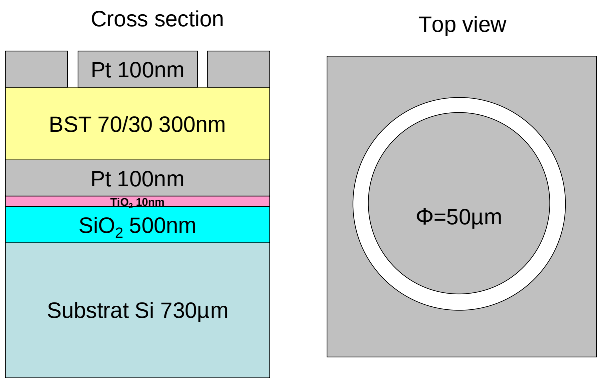

Figure 1: sketch of the technology developed: cross section and top view of the resonator

One has to note that this process requires only one mask design as proposed initially by Vorobiev et al. [3]. Therefore, this process limits considerably the negative influence of numerous technological steps on the final properties of BST. The main goal here is to try to figure out the potentiality of BST as an electroactive material, decoupled from the technological influence. Finally, a back side polishing is performed in order to enhance the substrate resonances.

III. MODEL

The design proposed allows taking into account the acoustic influence of the substrate underneath. Indeed, even if the active part comes from the BST layer, a lot of resonances are induced by the substrate as we will see in the experimental part. However, this structure permits extracting the properties of the BST layer by using an appropriate model.

This model was already developed for electrostrictive materials based resonators in the literature by several authors [1,2,4]. The assumption is that there is just one kind of acoustic wave that travelled trough the stack in the out-of-plane direction: the compression wave. Therefore, the model is reduced to one dimension, perpendicular to the layers plane. Here, we just adapted the model to this structure with the substrate. The main calculation step is to determine the electrical impedance of the BST layer by taking into account the mechanical and electrical conditions of the BST layer, which gives:

$$Z_{BST} = \frac{1}{jC_0 2\pi f}\left(1 - k_t^2 \frac{\tan\phi}{\phi} \frac{(z_{top} + z_{bot})\cos^2\phi + j\sin 2\phi}{(z_{top} + z_{bot})\cos 2\phi + j(z_{top} z_{bot} + 1)\sin 2\phi}\right) \qquad \text{Equation 1}$$

With C_0 the static capacitance of BST, f the frequency, k_t^2 the electromechanical coupling coefficient, $\phi = kt/2$ with k the wave vector and t the BST thickness, z_{top} and z_{bot} the normalized acoustic impedances seen by the BST respectively at the top and the bottom. Therefore, the top acoustical impedance is only represented by the top electrode influence whereas the bottom acoustical impedance is due to the contribution of the bottom electrode, the SiO_2 layer and the Si substrate. The TiO_2 layer is neglected here. The normalized impedances are calculated by the following relation:

$$z_{top} = \frac{Z_{top}}{Z_{BST}^0} \qquad z_{bot} = \frac{Z_{bot}}{Z_{BST}^0} \qquad \text{Equation 2}$$

where $Z_{BST}^0 = \sqrt{\rho_{BST} c_{BST}^D}$ the acoustic impedance of *BST*, ρ_{BST} and c_{BST}^D being respectively the density and the stiffness coefficient at constant displacement field of BST.

The final impedance of BST can be obtained by linking the influence of each layer to the BST layer. This is performed by respecting the boundaries conditions at each material interface. Indeed, at each interface, the mechanical conditions impose the equality of the acoustic impedance of the two layers involved. In the case of two successive materials said *n-1* and *n*, one can obtain that the impedance Z_n is the following [5]:

$$Z_n = Z_n^0 \left(\frac{Z_{n-1}\cos kd + jZ_n^0 \sin kd}{Z_n^0 \cos kd + jZ_{n-1}\sin kd}\right) \qquad \text{Equation 3}$$

d is the thickness of the layer n, $Z_n^0 = \sqrt{\rho_n c_n}$ is the acoustic impedance of the layer n (without the phase term compared to Z_n^0), k is the wave vector and Z_{n-1} is the impedance of the layer $n-1$. Therefore, this formula is useful to calculate the impedance successively from one layer to the next one. The beginning point should be the air interface and then the impedance is calculated until reaching the interface with BST. This allows obtaining z_{top} and z_{bot} involved in equation 1.

Finally, it is mandatory to introduce the electrostriction parameters into the expression of equation 1. This is done in the k_t^2 term. Indeed, for piezoelectric materials, k_t^2 is well defined from the piezoelectric coefficient, the dielectric constant and the stiffness coefficient. For the longitudinal mode, k_t^2 can take the expression $h^2/\beta^S c^D$ where h is the piezoelectric coefficient, β^S is the dielectric impermittivity at fixed *S (strain)* and c^D is the stiffness coefficient at fixed D [6]. The current idea to introduce the electrostrictive formalism is to start from the development of the free energy and then identify the terms corresponding to h, β^S and c^D. This is a thermodynamical way of doing. The free energy F form is the following:

$$F - F_0 = \frac{1}{2}c_0^D S^2 + \frac{1}{2}\beta^S D^2 + \frac{1}{4}\gamma^S D^4 + GD^2 S + \frac{1}{2}MS^2 D^2 \qquad \text{Equation 4}$$

Here, S is the strain, T the stress, D the electric displacement, E the electric field, c_0^D the stiffness coefficient without dc field, γ^S the non linear impermittivity, G the electrostrictive coefficient and M the non linear electrostrictive coefficient.

As $dF=TdS+EdD$, by differentiating F versus S and D, one obtain for T and E:

$$\begin{aligned} T &= c_0^D S + GD^2 + MSD^2 \\ E &= \beta^S D + \gamma^S D^3 + 2GSD + MS^2 D \end{aligned} \qquad \text{Equation 5}$$

If one adds a dc field superimposed to the ac field, one can deduce that after removing the constant dc terms:

$$\begin{aligned} T_{ac} &= \left(c_0^D + MD_{dc}^2\right)S_{ac} + \left(2GD_{dc} + 2MS_{dc}D_{dc}\right)D_{ac} \\ E_{ac} &= \left(\beta^S + 3\gamma^S D_{dc}^2 + 2GS_{dc} + MS_{dc}^2\right)D_{ac} + \left(2GD_{dc} + 2MS_{dc}D_{dc}\right)S_{ac} \end{aligned} \qquad \text{Equation 6}$$

The final step is to identify this form to the following one corresponding to the piezoelectric case:

$$\begin{aligned} T &= c^D S - hD \\ E &= \beta^S D - hS \end{aligned} \qquad \text{Equation 7}$$

Therefore, one obtains:

$$c^D = c_0^D + M\varepsilon^2 E_{dc}^2 \qquad \beta^S = \frac{1}{\varepsilon} \qquad -h = 2G\varepsilon E_{dc}\left(1 - \frac{M\varepsilon^2 E_{dc}^2}{c_0^D}\right) \qquad \text{Equation 8}$$

A supplementary model can be used to represent the dielectric constant as proposed by Chase et al. [7]:

$$\varepsilon(E) = \frac{\varepsilon_{\max}}{2\cosh\left(\frac{2}{3}\sinh^{-1}\left(2\frac{E}{E_{1/2}}\right)\right) - 1} \qquad \text{Equation 9}$$

Here, $E_{1/2}$ is the field for which the dielectric constant is equal to $\varepsilon_{max}/2$. This expression is often an efficient way to model the dielectric constant variation versus the dc field. Another possibility is to use a measured data file of the dielectric constant versus the field in equation 9.

Therefore, the final expression of the k_t^2 is:

$$k_t^2 \approx \frac{4G^2\varepsilon^3 E_{dc}^2}{c_0^D}\left(1 - \frac{2M\varepsilon^2 E_{dc}^2}{c_0^D}\right) \qquad \text{Equation 10}$$

Here, we supposed that the correction induced by the stiffness variation is negligible for the case of BST as the dielectric variation is around 50 times higher than the stiffness variation.

The losses in the model are taken into account by using the quality factor only in BST and the Si substrate. The following formulae are used [8]:

$$\phi_{BST} = \frac{kt}{2}\left(1 - i\frac{1}{2Q_{BST}}\right)$$

$$\phi_{Si} = k_{Si}t_{Si}\left(1 - i\frac{1}{2Q_{Si}}\right) = \frac{wt_{Si}}{v_{Si}}\left(1 - i\frac{1}{2Q_{Si}}\right) \qquad \text{Equation 11}$$

IV. CHARACTERIZATION

The impedance of the BST layer is calculated from the complex S_{11}-parameter measured with a Vectorial Network Analyser (VNA). The design allows a 1-port measurement by using GSG probes with the S probe touching the central circle as observed in Figure 1. The curves of the impedance module obtained with different dc voltage are shown in figure 2. At 0V, the Z module looks like a capacitor ($Z=1/C_0 2\pi f$). When the dc voltage increases, one can observe two phenomena: first, for a given frequency, the impedance increases. This is due the decrease of the dielectric constant versus dc bias as it is well known in perovskite materials. The second effect is the occurrence of a resonance and antiresonance at a given frequency in the 3.5-4 GHz range. The peaks intensity increases with the dc field. This is linked to the electromechanical coupling due to the electrostrictive properties of BST. The peaks are broad. It is an evidence of the substrate effect: a lot of close harmonics are superimposed.

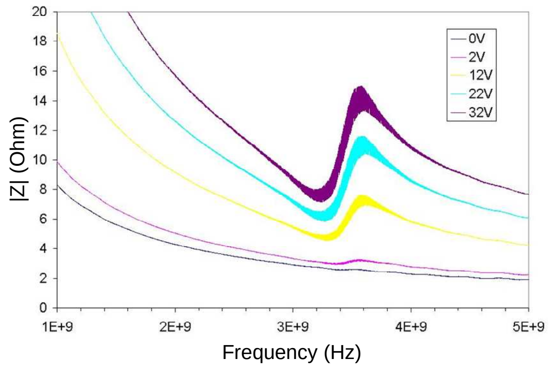

Figure 2: impedance module of the BST resonator versus frequency at different dc bias

The model is therefore fitted to the experimental curve. The results at 32V dc bias are shown in figure 3. The real parts of the impedance and the admittance are very well reproduced by the model.

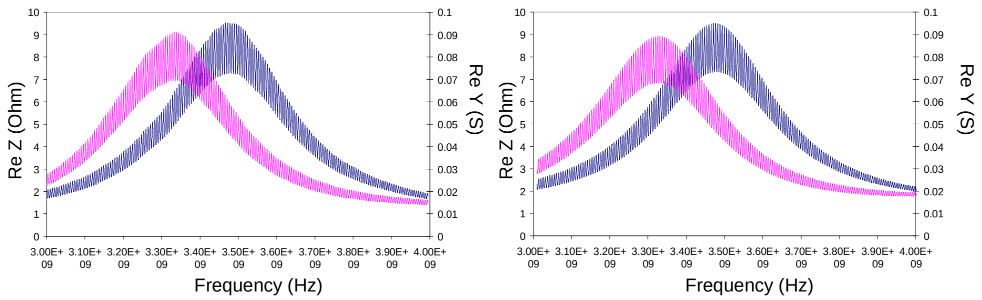

Figure 3: real part of the impedance (blue) and the admittance (pink) of the BST at 32 V dc bias - top: measurement – bottom: model

The parameters used in the model at different voltages are shown in the figure 4.

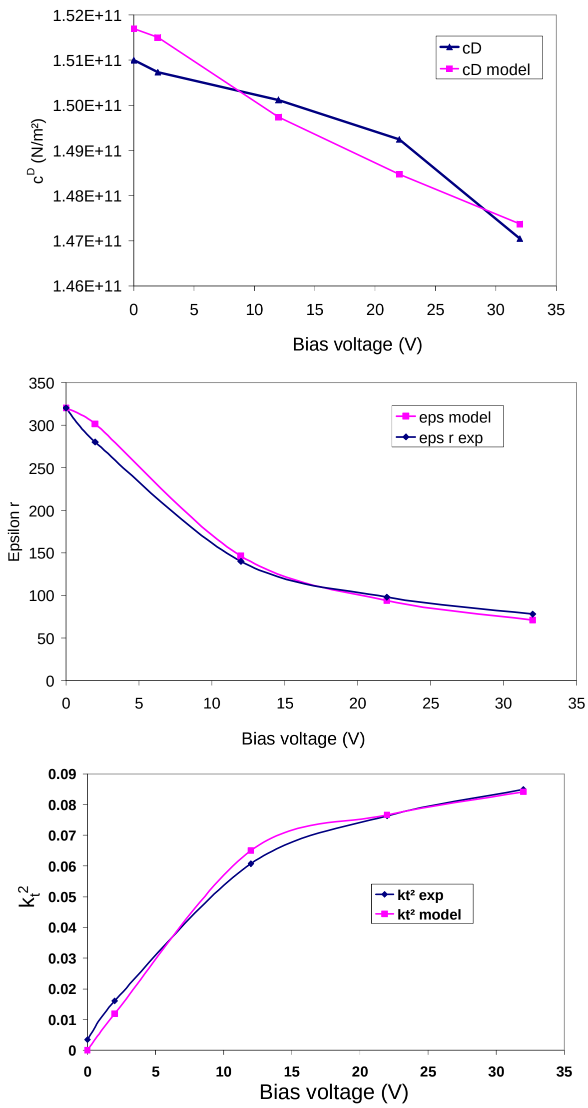

Figure 4: c^D , ε_r and k_t^2 extracted from the model after fitting the experiment versus dc bias

For all the extracted data, a Q_{Si} of 2000 was used. The Q_{BST} cannot be properly extracted by using this structure as the substrate strongly influences the resonance of the BST alone. The stiffness variation reaches 2.6% inducing an antiresonance frequency reaching -1.7%. Besides, the maximum k_t^2 reaches 8.5% for a high electric field ($1.07.10^8$V/m). This value is higher than the one exhibited by AlN.

Finally, these features are used to simulate the behaviour of a filter involving two BST resonators in the FBAR configuration, without the substrate influence. The design is the simple 1-stage ladder one simulated at different voltages. The result is shown in figure 5. It is interesting to note that once at least 10V is applied, the bandwidth BW of the filter is quite constant. The central frequency of the filter shifts towards the lower frequencies when the dc bias increases. The shift obtained when the BW is constant reaches the 1% range at 30V. Although the equivalent field is high (1MV/cm), the shift is significant and could allows to address for instance the technological drift of the thickness deposition.

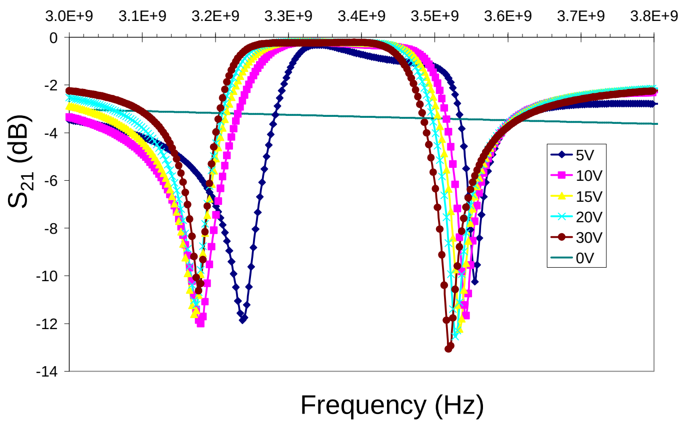

Figure 5: simulation of a one-stage ladder design involving 2 BST FBAR resonators

V. CONCLUSION

This study based on a simple structure constituted by an active layer, its electrodes and a substrate underneath proves that BST can exhibit a high electromechanical coupling reaching 8.5% which is higher than Aluminium Nitride, the standard material for acoustic resonators in the GHz frequency range. A final simulation shows that tunable passband filters could be obtained by using dc controlled BST based resonators. It appears that there is a dc voltage domain where the bandwidth is quite constant. Therefore, the filter central frequency can be adjusted by changing the dc field independently from the bandwidth. The frequency tuning achievable reaches 1 % with 30V dc with a central frequency at 3.5GHz. Due to non negligible second order effects as electrostriction, dielectric and stiffness non linearities, BST exhibits tunable behaviours which is highly desirable for tunable filters.

REFERENCES

[1] Andreas Noeth, Tomoaki Yamada, Vladimir O. Sherman, Paul Muralt, Alexander K. Tagantsev, and Nava Setter, Tuning of direct current bias-induced resonances in micromachined Ba0.3Sr0.7TiO3 thin-film capacitors, Journal of Applied Physics 102, 114110 (2007)

[2] S. Gevorgian, A. Vorobiev, T. Lewin, *J. Appl. Phys.*, 99, 124112 (2006)

[3] A. Vorobiev, P. Rundqvist, K. Khamchane, S. Gevorgian, *Appl. Phys. Lett.*, 83 (15), 3144 (2003)

[4] Volatier-A; Defay-E; Aid-M; Nhari-A; Ancey-P; Dubus-B, Switchable and tunable strontium titanate electrostrictive bulk acoustic wave resonator integrated with a Bragg mirror, *Applied Physics Letters*.; 92(3): 032906 (2008

[5] Lakin et al ; High Q microwave acoustic resonators and filters, *IEEE Transactions on microwave theory and techniques*, vol. 41, N°12 (1993), 2139-2146

[6] IEEE Standard on Piezoelectricity, ANSI/IEEE Std 176-1987

[7] D.R. Chase, Lee-Yin Chen, R.A. York, Modeling the capacitive non linearity in thin film BST varactors, *IEEE transactions on microwave theory and techniques*, vol. 53 (10), p.3215 (2005).

[8] Roman Lanz, PhD thesis, Ecole Polytechnique de Lausanne (2004)